Development of a Wire Mesh Composite Material for Aerospace Applications

Siva Chakra Avinash Bikkina
Department of Electrical, Electronics and Communication Engineering, GITAM Deemed to be University
Visakhapatnam, India
sbikkina@gitam.in

Pappu V. Y. Jayasree
Department of Electrical, Electronics and Communication Engineering, GITAM Deemed to be University
Visakhapatnam, India
jpappu@gitam.edu

Received: 13 July 2022 | Revised: 9 August 2022 | Accepted: 14 August 2022

Abstract-The electrical conductivity of Fiber-Reinforced Polymers (FRPs) may be used to reduce the dangers of lightning strikes, radar radiation, and aerial radio frequency transmitters. Metal Matrix Composites (MMCs) were created to guard against Electromagnetic Interference (EMI) in the aircraft's electric and electrical systems. High-Intensity Radiated Field Protection (HIRFP) aircrafts are required to be manufactured from a metal matrix consisting of Al6061, Al2O3, and Fly Ash (FA) to keep up with the ever-increasing needs of industry. The current work considered three MMC combinations. MMC1 is AL6061+10% and Al2O3+5% FA, MMC2 consists of AL6061+15 and Al2O3+5% FA, and MMC3 of AL6061+20% and Al2O3+5% FA. These MMCs made the shielding more effective at different percentages. The material electrical properties were interpreted based on experiments. Analytical approaches include the testing of the electrical parameters of materials to measure the shielding effectiveness. The calculated shielding efficiencies MMC1-55.7dB, MMC2-57.2dB, and MMC3-59.1dB allow the composites to be employed in aircrafts. This indicates that, for specific applications like HIRFPs, the constructed MMCs perform well.

Keywords-Metal Matrix Composites (MMCs); reinforcement; Al_2O_3; fly ash

I. INTRODUCTION

Frequent lightning strikes can harm commercial airliners. Lightning's high-intensity fields interfere with the electronic devices of the in-built guidance and communication systems [1-2]. The damage caused by lightning to aircrafts varies significantly with altitude and flight duration [3]. With its precise rigidity, strength, and lightweight, FRPs are ideal for aircraft reinforcement [4]. The materials used in their construction have sufficient mechanical qualities and low energy consumption per unit. However, they have low electrical conductivity, and the electric field cannot travel through it, resulting in delamination and embrittlement when lightning hits an aircraft [5]. Aluminum composites have great promise since their fundamental qualities may be enhanced by reinforcing with other materials. Metals including titanium, nickel, magnesium, copper, and aluminum have all been utilized to create metal matrix composites. As a result of its low density, high strength, low electrical conductivity, and high reflectivity, aluminum is the material of choice [6]. Authors in [7] studied various physical models based on the electrical qualities of lightning strike protection. With its low density, particular corrosion resistance, high strength, and solid electrical qualities, Al6061 was developed as an alternative to FRPs [8]. Since many incident EM waves are arbitrarily oriented, an evaluation of wire mesh's shielding effectiveness for normal incidence might be generalized to all practical applications. The study is based on TL modelling in the situation of normal incidence. It is an arbitrary perspective because the polarized electric and magnetic fields in this situation are normal or vertical to the plane. The referenced research analyzed the oblique impact of lightning's EM waves on aircraft. Authors in [9] created a lightning-proof carbon filter epoxy pre-preg laminate with a 55dB SE.

The novelty of the proposed research work is the protection of the electronic components of the aircraft from the lightning strike effect. To protect from this effect, a MMC (Al6061) with a variety of Al_2O_3/FA particle reinforced was considered. Electrical conductivity, permeability, and permittivity were measured after reinforcing Al6061 with varying concentrations of considered and 5% FA. The shielding effectiveness of the composite material was calculated with the TL method. Simulations were performed to determine the efficiency of shielding against X-band electromagnetic radiation with oblique incidence. The whole process was well-organized, from the preparation of the materials to the efficiency assessment of the shielding, and to result analysis.

II. UTILIZED MATERIALS

Aluminum oxide (Al_2O_3) has a density of 0.0039kg/cc^3, and is employed as a reinforcing material because of its high corrosion resistance and high-temperature tolerance. As a result, the Al_2O_3 particles in hybrid composites are also used as load-bearing and electrical conductivity components in metals. Al_2O_3 and Al6061 may be used in aircraft design because of their low cost [10-11]

FA is a byproduct of coal-fired thermal power plants. In recent decades, carbon fibers have been used as a reinforcing material for aluminum-based metal matrix composites. To prevent Al_4C_3, FA may be used for aluminum metal matrix composites reinforced with silicon carbide (SiC) [14]. A

Corresponding author: Siva Chakra Avinash Bikkina

substance's absorption capacity may be increased to enhance the shielding qualities of the substance. Only 5% FA may be utilized in the composite since it affects the material's tensile strength [12-13].

III. COMPOSITE MATERIAL PREPARATION

As indicated in Figure 1, stir casting was used to add micro-sized Al_2O_3 and FA to the Al6061 metal matrix composite to improve its electrical and mechanical characteristics. A composite is formed when two or more materials are combined, as shown in Table I. The fabricated materials made from stir casting are shown in Figure 2. Stir casting is the most cost-effective technique for synthesizing particle-reinforced composites, and this is how the proposed MMC is made. A furnace, a feeder for reinforcing ingredients, and a stirrer were used in the stir casting process to create the composite. The stirrer comes with a rod and blades for stirring. A resistance-heated muffle furnace was used to heat 1kg of Al6061 alloy to 720°C in a ceramic crucible. Before casting, the Al 6061 alloy was warmed to 600°C to remove any gases and moisture from the reinforcing particles (Al_2O_3 and FA). This prevents temperature drops during the casting process. The stirrer's alumina-coated blades are used to avoid ferrous ions.

Fig. 1. Experimental setup for reinforcement using stir casting.

Fig. 2. Fabricated material from stir casting.

FA (5wt%) and varied quantities of Al_2O_3 (5wt%) were used to make the composites described in Table I. The liquid composite was mixed with all the reinforcing elements and was then poured into a steel mold warmed to 250°C to prevent condensation from forming. The metal cools in the atmosphere before solidifying. The mold was emptied of the solidified composite. The other specimens were made with the same process but with varied quantities of reinforcing materials.

TABLE I. METAL MATRIX REPRESENTATION

Material and weight percentages combined	Representation
AL6061+10% Al_2O_3+5% FA	MMC-1
AL6061+15% Al_2O_3+5% FA	MMC-2
AL6061+20% Al_2O_3+5% FA	MMC-3

IV. ELECTRICAL PARAMETER CALCULATION

The Transmission/Reflection method utilized by a E8263B Agilent Technologies Vector Network Analyzer (VNA) was used to determine the permeability (μ), permittivity (ε), and conductivity (σ), of the MMCs (Figure 3). In order to create the incident electromagnetic wave, a piece of MMC was put into the waveguide [14-15]. To analyze the electrical properties of the composite, a waveguide measuring 22.86mm × 10.16mm was implanted in the test specimens. The MMC samples utilized in the waveguide are shown in Figure 2, and the experimental setup for the transmission/reflection approach is shown in Figure 3. We conducted the experiment in the X-band and determined the VNA levels for a range of frequencies. The results of the VNA are shown in Figures 6–9. They provide evidence that μ, σ, and ε have a connection to periodicity. It is important to note that the electrical characteristics of MMC vary with its operating frequency. The degree to which a given material may operate as a shield depends on the values of μ, σ, and ε in the MMC ratio.

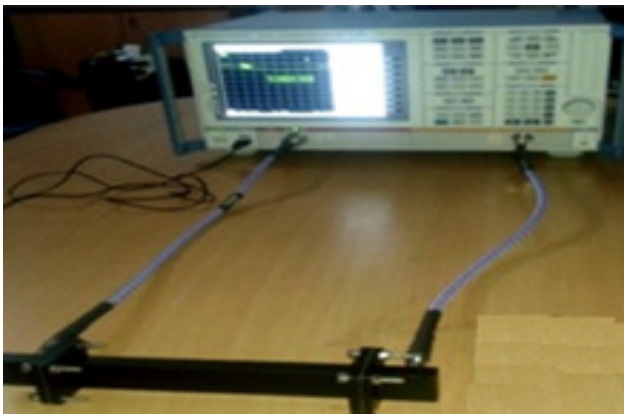

Fig. 3. Transmission/Reflection method experimentatal setup.

V. THEORETICAL ANALYSIS OF SHIELDING EFFECTIVENESS FOR WIRE MESH METAL MATRIX COMPOSITES

The Shielding Efficiency (SE) [17] statistic is often used to evaluate a material's shielding capacity. Figure 4 shows the mesh surface with an oblique incidence of electromagnetic (EM) waves [16]. The mesh surface with an oblique incidence of EM wave is shown in Figure 4. The ratio of received power before and after shielding is used to quantify EM shielding effectiveness. In (1), p_r represents the received power before the area was shielded, and p_s represents the measured power after the region was shielded. The same approach is used to protect against electric and magnetic fields and is effective in both application circumstances.

$$SE(dB) = 10\log_{10}\left(\frac{p_r}{p_s}\right) \quad (1)$$

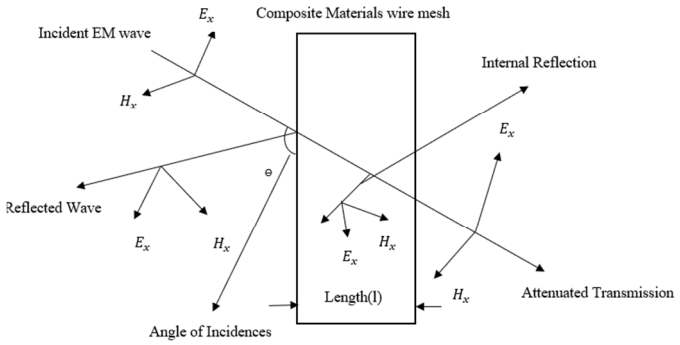

Fig. 4. Representation of oblique incidences for WMMMC.

Simple in design, the Wire Metal Matrix Mesh Composite (WMMMC) is made up of parallel MMC wires that are equally spaced apart. This means that the effectiveness of WMMMC as a radiation shield depends on parameters such as the distance between the wires, their thickness, the wave's incidence angle, etc. It is possible to increase the SE of such a mesh by using additional orthogonal wires to the initial set of wires. Electromagnetic shielding effectiveness is examined when mesh apertures are small in contrast to the operating wavelength of the screen. The impedance of a wire-mesh screen sheet is used to measure its impedance [18-19]. When an electromagnetic wave with a relatively low frequency strikes a mesh, a reactive field is formed near the mesh surface. Without a screen, this reactive field diminishes exponentially with distance [19]. As can be seen in Figure 1 of [22], a mesh with a square aperture length a_s and wire radius r_w has a shielding efficacy [20-22] that may be defined as:

$$z_{s1} = z'_w a_s + j\omega L_S \quad (2)$$

$$z_{s2} = z_s - \frac{j\omega L_S}{2} sin\theta^2 \quad (3)$$

The following calculations show that the transmission coefficients for polarization T_1 and T_2 represent TE and TM modes and can be calculated for a range of frequencies and incidence angles.

$$T_1 = \frac{2\left(\frac{z_{S1}}{z_0}\right)cos\theta}{1+2\left(\frac{z_{S1}}{z_0}\right)cos\,\theta} \quad (4)$$

$$T_2 = \frac{2\left(\frac{z_{S2}}{z_0}\right)cos\theta}{1+2\left(\frac{z_{S2}}{z_0}\right)cos\theta} \quad (5)$$

where θ is the incidence angle, calculated from the flat sheet's regular, z_o is the free-space impedance, and z_{s1} and z_{s2} are the eigenvalues of TE and TM mesh impedance operators respectively. The sheet inductance L_s is calculated from:

$$L_s = \frac{\mu_0 . a_s}{2\pi} \ln(1 - e^{-\frac{2\pi r_s}{a_s}})^{-1} \quad (6)$$

The wire impedance per unit length z'_w depends on the resistance per unit length, τ_w is a time constant and I_0 and I_1 are first kind Bessel functions.

$$z'_w = r'_w \frac{(\sqrt{jw\tau_w}).I_0.(\sqrt{jw\tau_w})}{2.I_1.(\sqrt{jw\tau_w})} \quad (7)$$

$$SE = -10log_{10}\left(\left(\frac{1}{2}T_1^2\right) + \left(\frac{1}{2}T_2^2\right)\right) \quad (8)$$

$$T_{total} = -SE \quad (9)$$

Since no noticeable change occurred for the frequencies and structures under examination when the skin effect was included in (7), the DC wire resistance was included as an approximation to the wire impedance (6). Consequently, it becomes straightforward to determine the SE of a particular mesh (with square openings) under various situations (and in different directions).

VI. SIMULATION RESULTS

A. Electrical Parameter Measurements

The connection between an electrical parameter of a composite material and its frequency may be deduced from the vector analyzer's output considering the electrical characteristics of conductivity, permeability, and permittivity. As a direct result of the material's permeability and permittivity, its electrical properties are intimately linked. The essential portion of the permittivity of lossless materials displays the quantity of stored electrical energy.

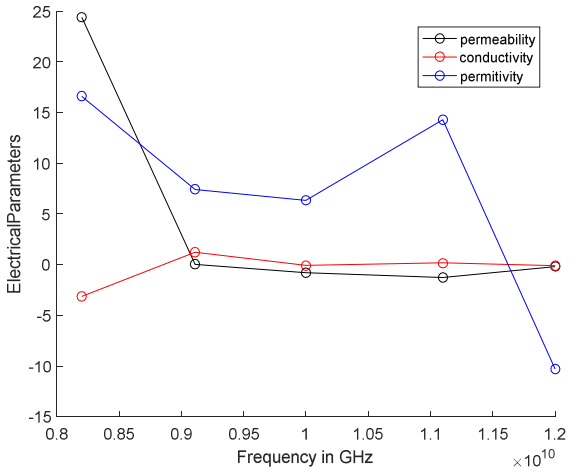

Fig. 5. Electrical parameters of pure AL6061.

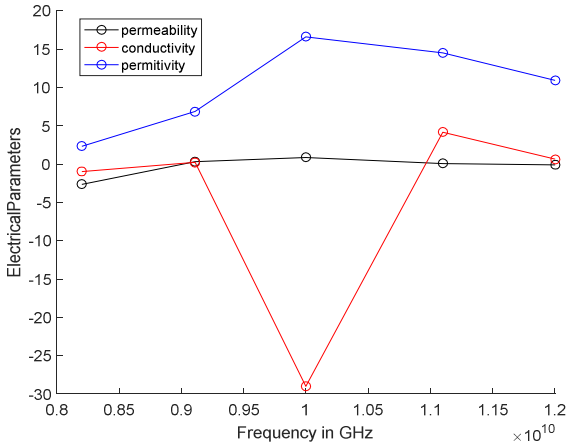

Fig. 6. Electrical parameters of MMC-1.

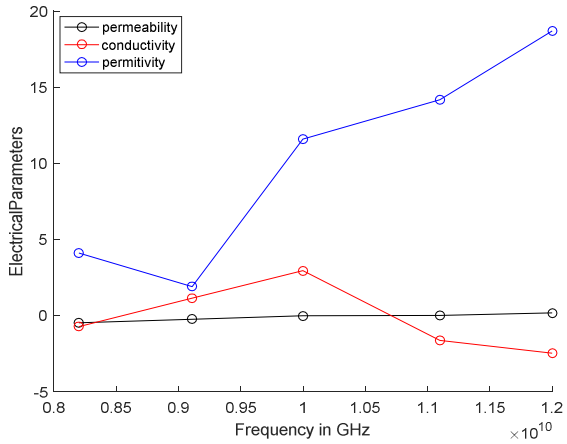

Fig. 7. Electrical parameters of MMC-2.

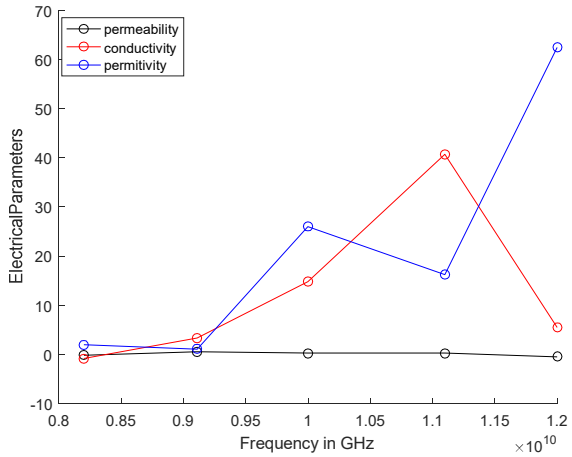

Fig. 8. Electrical parameters of MMC-3.

The imaginary part of permeability is used to quantify the power lost due to magnetic fields, which is crucial for calculating the magnetic energy stored in a material. A VNA having a waveguide or coaxial construction and working at 8–12GHz may be used to assess scattering properties (X-band frequency). To calculate the reflection coefficient equation's value, |S11| and |S21| were plugged into the calculator's bar. The VNA results are shown in Figures 5-8.

B. Shielding Effectiveness Mesearument

Most electromagnetic signal occurrences on the mesh surface were oblique in practice, as described in the literature. Using a range of angles from 0 to 90°, the shielding performance of each composite was evaluated. As the incidence angle increases, so does the shielding, as shown by the relationship between the electromagnetic mesh surface and the incidence angle. The stimulated results of pure AL6061 and MMC are represented in Figures 9-12. At increasing incidence angles, the shielding efficiency of pure AL6061 and composites supported by varying proportions of Al_2O_3 and FA as shown in Table II. SE decreases as the incidence angle becomes normal to the mesh material. Al_2O_3 and FA have been used in this study to support AL6061 alloys. Shielding relies on absorption and reflection for its success. Permeability may be used to measure the material's ability to absorb. Depending on the conductivity of the substance, the reflectance of the object changes. The material's excellent permeability and conductivity result in high absorption and reflection losses. The composite material's permittivity improves as a result of the Al_2O_3 growing proportion. Also, the whole composite's absorption loss rises. For aviation applications of 48.83dB, the effective shielding effectiveness is considered adequate [29-30]. The material's excellent permeability and conductivity result in high absorption and reflection losses. The composite's 55.7dB shielding value at a 20° angle of incidence aided by Al_2O_3 (10%) and FA (5%) reinforcement resulted in reflection and only absorption from the FA. By increasing the Al_2O_3 and FA content by 15% and 20%, 57.6dB and 59.1dB increase in shielding value is respectively obtained. The material will no longer be suitable for aviation applications if the percentage exceeds that level.

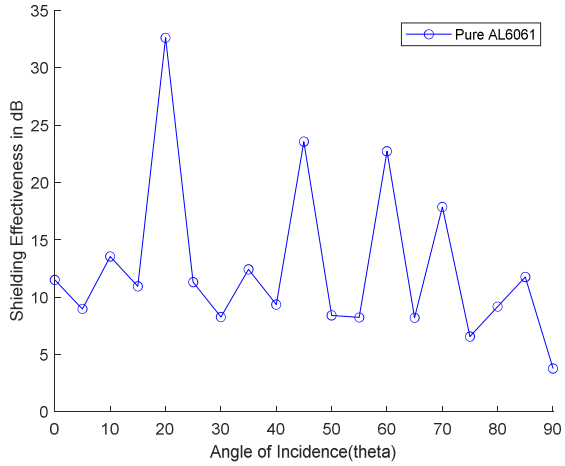

Fig. 9. Shielding effectiveness of pure AL6061.

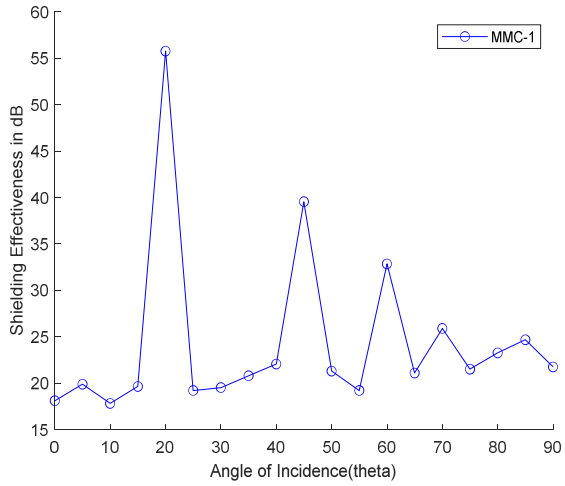

Fig. 10. Shielding effectiveness of MMC-1.

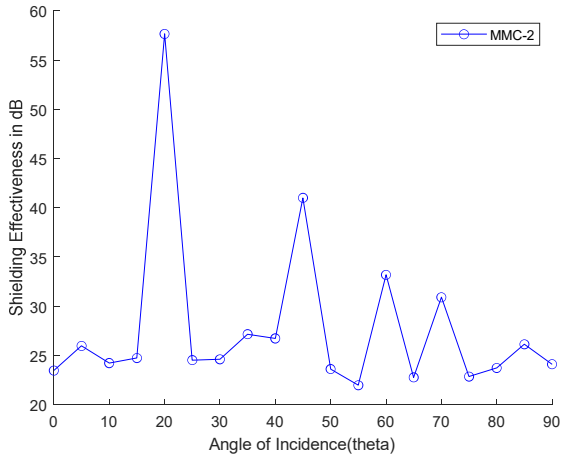

Fig. 11. Shielding effectiveness of MMC-2.

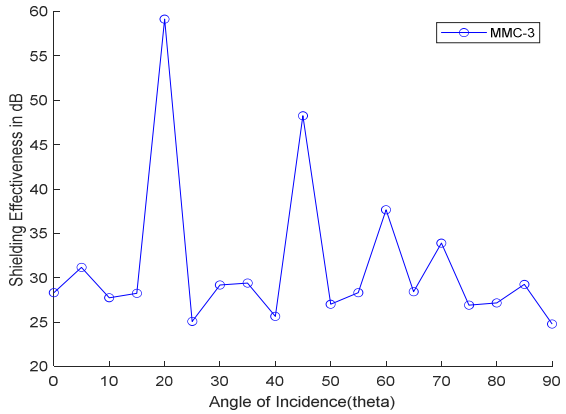

Fig. 12. Shielding effectiveness of MMC-3.

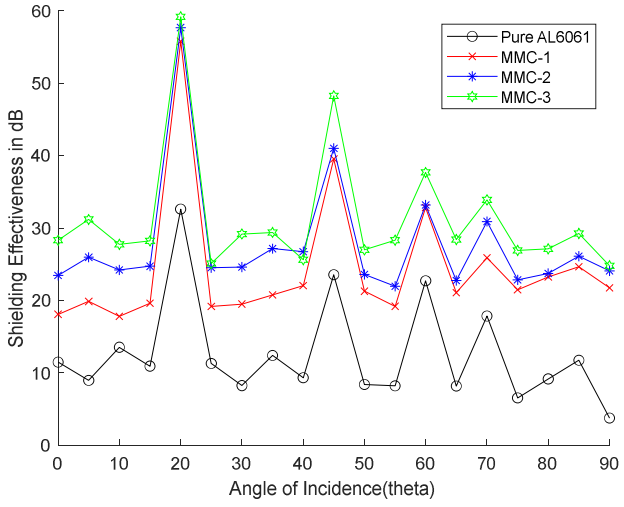

Fig. 13. Shielding effectiveness comparison of MMCs with Pure AL6061.

The FA content of all combinations is fixed to 5%. If the concentration is more, the material strength decreases, and the material properties are lost. Shielding increases by around 20% for incidence angles of 45°, 60°, 70°, and 85°, but as the incidence angle increases, the values decrease. Table II shows the comparison of the results of the present work with other known works and Table III exhibits the shielding effectiveness of MMCs with different angle of incidences.

TABLE II. COMPARISON OF SHIELDING EFFECTIVENESS VALUES

Reference	Material	Frequncy	Shielding effectiveness
[23]	Al_2O_3/FeSiAl/flaky graphite	X band	30.4
[24]	$Ti_3Si(Al)C_2/Al_2O_3$	X band	42.1
[25]	Al_2O_3	X band	29-32
Present work	Al6061/ Al_2O_3/FA	X band	59.1

TABLE III. RELATIONSHIP BETWEEN THE SHIELDING PROPERTIES OF VARIOUS REINFORCED MATERIALS AND AL6061 COMPOSITE AT VARIOUS INCIDENCE ANGLES

	Incidence angle				
Material	**20°**	**45°**	**60°**	**70°**	**85°**
Pure AL6061	32.62	23.48	22.72	17.86	11.77
MMC-1	55.7	39.5	32.8	25.8	24.6
MMC-2	57.6	41	33.1	30.9	26.17
MMC-3	59.1	48.2	37.6	33.8	29.3

VII. CONCLUSION

Composite materials with strong SE are well-known in aerial applications. The WMCs developed in this work will give SE up to 59.1dB. Electromagnetic shielding is evaluated from different perspectives (20°, 45°, 60°, 70°, and 85°). These MMCs have an SE of more than 55dB. So, these materials are more suitable for protecting aircrafts from lightning strikes. MMCs structure has physical flexibility and less weight, so they are more suited to protect large structures than metal sheets. Compared to metal-coated windows, wire mesh screens offer a unique advantage. The proposed WMMMC has lower SE than metallic sheets. According to the literature, using a material with a 50dB shielding efficiency for aircraft surfaces provides good lightning protection. Regarding high-intensity radiation fields, the shielding of prepared compositions may be used in airborne radars and wind turbine systems. Any mix of materials may be employed to satisfy the demands of different applications. A variety of aluminum composite materials may be treated to provide the appropriate shielding.

REFERENCES

[1] M. A. Uman and V. A. Rakov, "The interaction of lightning with airborne vehicles," *Progress in Aerospace Sciences*, vol. 39, no. 1, pp. 61–81, Jan. 2003, https://doi.org/10.1016/S0376-0421(02)00051-9.

[2] A. Larsson, "The interaction between a lightning flash and an aircraft in flight," *Comptes Rendus Physique*, vol. 3, no. 10, pp. 1423–1444, Dec. 2002, https://doi.org/10.1016/S1631-0705(02)01410-X.

[3] M. Jaroszewski, S. Thomas, and A. V. Rane, "Recent progress in electromagnetic absorbing materials," in *Advanced Materials for Electromagnetic Shielding: Fundamentals, Properties, and Applications*, New York, NY, USA: John Wiley & Sons, 2018, pp. 147–166.

[4] Y. Guo, Y. Xu, Q. Wang, Q. Dong, X. Yi, and Y. Jia, "Eliminating lightning strike damage to carbon fiber composite structures in Zone 2 of aircraft by Ni-coated carbon fiber nonwoven veils," *Composites Science and Technology*, vol. 169, pp. 95–102, Jan. 2019, https://doi.org/10.1016/j.compscitech.2018.11.011.

[5] M. Gagne and D. Therriault, "Lightning strike protection of composites," *Progress in Aerospace Sciences*, vol. 64, pp. 1–16, Jan. 2014, https://doi.org/10.1016/j.paerosci.2013.07.002.

[6] G. Moona, R. Walia, R. Vikas, and R. Sharma, "Aluminium metal matrix composites: A retrospective investigation," *Indian Journal of Pure and Applied Physics*, vol. 56, pp. 164–175, Jan. 2018.

[7] Z. M. Gizatullin, R. M. Gizatullin, and M. G. Nuriev, "Technique of physical modeling of lightning strike effects on aircraft," *Russian Aeronautics (Iz VUZ)*, vol. 59, no. 2, pp. 157–160, Apr. 2016, https://doi.org/10.3103/S106879981602001X.

[8] B. V. Ramnath *et al.*, "Aluminium metal matrix composites–A review," *Reviews on Advanced Materials Science*, vol. 38, pp. 55–60, 2014.

[9] B. Zhang, S. A. Soltani, L. N. Le, and R. Asmatulu, "Fabrication and assessment of a thin flexible surface coating made of pristine graphene for lightning strike protection," *Materials Science and Engineering: B*, vol. 216, pp. 31–40, Feb. 2017, https://doi.org/10.1016/j.mseb.2017.02.008.

[10] V. V. Vani and S. K. Chak, "The effect of process parameters in Aluminum Metal Matrix Composites with Powder Metallurgy," *Manufacturing Review*, vol. 5, 2018, Art. no. 7, https://doi.org/10.1051/mfreview/2018001.

[11] G. Pitchayyapillai, P. Seenikannan, K. Raja, and K. Chandrasekaran, "Al6061 Hybrid Metal Matrix Composite Reinforced with Alumina and Molybdenum Disulphide," *Advances in Materials Science and Engineering*, vol. 2016, Nov. 2016, Art. no. e6127624, https://doi.org/10.1155/2016/6127624.

[12] A. Dey and K. M. Pandey, "Characterisation of fly ash and its reinforcement effect on metal matrix composites: A review," *Reviews on Advanced Materials*, vol. 44, pp. 168–181, 2016.

[13] A. K. Senapati, P. C. Mishra, and B. C. Routara, "Use of Waste Flyash in Fabrication of Aluminium Alloy Matrix Composite," *International Journal of Engineering and Technology*, vol. 6, no. 2, pp. 905–912, 2014.

[14] U. C. Hasar, "Permittivity Measurement of Thin Dielectric Materials from Reflection-Only Measurements Using One-Port Vector Network Analyzers," *Progress In Electromagnetics Research*, vol. 95, pp. 365–380, 2009, https://doi.org/10.2528/PIER09062501.

[15] A. P. Alegaonkar and P. S. Alegaonkar, "Nanocarbons: Preparation, assessments, and applications in structural engineering, spintronics, gas sensing, EMI shielding, and cloaking in X-band," in *Nanocarbon and its Composites*, A. Khan, M. Jawaid, Inamuddin, and A. M. Asiri, Eds. Sawston, UK: Woodhead Publishing, 2019, pp. 171–285.

[16] L. F. Liu and Q. S. Zhang, "Analysis of Electromagnetic Shielding Effectiveness of Metal Material," *Advanced Materials Research*, vol. 538–541, pp. 655–659, 2012, https://doi.org/10.4028/www.scientific.net/AMR.538-541.655.

[17] D. Mansson and A. Ellgardt, "Comparing analytical and numerical calculations of shielding effectiveness of planar metallic meshes with measurements in cascaded reverberation chambers," *Progress In Electromagnetics Research C*, vol. 31, pp. 123–135, 2012, https://doi.org/10.2528/PIERC12061506.

[18] P. S. Spandana and P. V. Y. Jayasree, "A Mathematical Approach to the Effect of Mobile Position on Human Head Against RF Radiation," *Progress In Electromagnetics Research C*, vol. 121, pp. 127–144, 2022, https://doi.org/10.2528/PIERC22051604.

[19] P. S. Spandana and P. V. Y. Jayasree, "Numerical Computation of SAR in Human Head with Transparent Shields Using Transmission Line Method.," *Progress In Electromagnetics Research M*, vol. 105, pp. 31–45, Jul. 2021.

[20] K. F. Casey, "Electromagnetic shielding behavior of wire-mesh screens," *IEEE Transactions on Electromagnetic Compatibility*, vol. 30, no. 3, pp. 298–306, Dec. 1988, https://doi.org/10.1109/15.3309.

[21] S. S. Pudipeddi, P. V. Y. Jayasree, and S. G. Chintala, "Polarization Effect Assessment of Sub-6 GHz Frequencies on Adult and Child Four-Layered Head Models," *Engineering, Technology & Applied Science Research*, vol. 12, no. 4, pp. 8954–8959, Aug. 2022, https://doi.org/10.48084/etasr.5096.

[22] H. M. El-Maghrabi, "Electromagnetic Shielding Effectiveness Calculation for Cascaded Wire-Mesh Screens with Glass Substrate," *The Applied Computational Electromagnetics Society Journal*, vol. 33, no. 6, pp. 641–647, 2018.

[23] L. Zhou *et al.*, "Dielectric properties and electromagnetic interference shielding effectiveness of Al2O3-based composites filled with FeSiAl and flaky graphite," *Journal of Alloys and Compounds*, vol. 829, Jul. 2020, Art. no. 154556, https://doi.org/10.1016/j.jallcom.2020.154556.

[24] N. Dong *et al.*, "Fabrication and electromagnetic interference shielding effectiveness of Ti3Si(Al)C2 modified Al2O3/SiC composites," *Ceramics International*, vol. 42, no. 8, pp. 9448–9454, Jun. 2016, https://doi.org/10.1016/j.ceramint.2016.03.001.

[25] L. Zhu *et al.*, "Significantly enhanced electromagnetic interference shielding in Al2O3 ceramic composites incorporated with highly aligned non-woven carbon fibers," *Ceramics International*, vol. 45, no. 10, pp. 12672–12676, Jul. 2019, https://doi.org/10.1016/j.ceramint.2019.03.079.